SANDIA REPORT

SAND95–0758 • UC–706
Unlimited Release
Printed June 1995

Final Report
Non-Invasive Current and Voltage Imaging Techniques for Integrated Circuits Using Scanning Probe Microscopy
LDRD Project (FY93 and FY94)

Ann N. Campbell, Edward I. Cole, Jr., Paiboon Tangyunyong

Prepared by
Sandia National Laboratories
Albuquerque, New Mexico 87185 and Livermore, California 94550
for the United States Department of Energy
under Contract DE-AC04-94AL85000

Issued by Sandia National Laboratories, operated for the United States Department of Energy by Sandia Corporation.

Available to DOE and DOE contractors from
Office of Scientific and Technical Information
PO Box 62
Oak Ridge, TN 37831

Prices available from (615) 576-8401, FTS 626-8401

Available to the public from
National Technical Information Service
US Department of Commerce
5285 Port Royal Rd
Springfield, VA 22161

NTIS price codes
Printed copy: A03
Microfiche copy: A01

DISCLAIMER

SAND95-0758
Unlimited Release
Printed June 1995

Distribution
Category UC-706

Final Report
Non-Invasive Current and Voltage Imaging Techniques for Integrated Circuits Using Scanning Probe Microscopy LDRD PROJECT (FY93 and FY94)

Ann N. Campbell, Edward I. Cole, Jr., andPaiboon Tangyunyong
Sandia National Laboratories
Failure Analysis Department
Albuquerque, NM 87185-1081

ABSTRACT

This report describes the first practical, non-invasive technique for detecting and imaging currents internal to operating integrated circuits (ICs). This technique is based on magnetic force microscopy and was developed under Sandia National Laboratories' LDRD (Laboratory Directed Research and Development) program during FY 93 and FY 94. LDRD funds were also used to explore a related technique, charge force microscopy, for voltage probing of ICs. This report describes the technical work performed under this LDRD as well as the outcomes of the project in terms of publications and awards, intellectual property and licensing, synergistic work, potential future work, hiring of additional permanent staff, and benefits to DOE's defense programs (DP).

TABLE OF CONTENTS

NOMENCLATURE

AFM - atomic force microscopy
CFM - charge force microscopy
DOE - U. S. Department of Energy
DP - Defense Programs (U. S. Department of Energy)
IC - integrated circuit
MFM - magnetic force microscopy
MFM/CCI - magnetic force microscopy/current contrast imaging
SFM - scanning force microscopy
SPM - scanning probe microscopy

OVERVIEW

This report describes the work performed under the Sandia National Laboratories LDRD project titled "Non-Invasive Current and Voltage Imaging Techniques for Integrated Circuits Using Scanned Probe Microscopy." This project addresses the need for the development of an advanced integrated circuit analysis technique for non-invasive detection and imaging of currents in integrated circuit (IC) conductors. These techniques are required for failure analysis as well as design verification and model validation of ICs. Magnetic force microscopy (MFM) was selected for performing current imaging because of its high sensitivity as well as the excellent spatial resolution which can be achieved with scanning probe microscopy (SPM) based techniques. We demonstrated for the first time that MFM can be used to detect and image ac currents in ICs with a sensitivity of 1 mA dc and 1 μA ac. In addition, we implemented charge force microscopy (CFM), an SPM-based technique for detecting voltages, and applied CFM in order to image voltages on integrated circuit conductors. We achieved a submicron spatial resolution for both current and voltage imaging.

Our experimental approach and results are described in detail in this report. We also discuss the development of a large area scanning capability for localizing the elevated current paths on an entire IC. This approach uses a translation stage rather than the x and y piezoelectric drivers to quickly scan the entire die and overcomes the limitations of constructing a mosaic of images of smaller areas to obtain a large area image. In addition, we describe an approach that could be used for obtaining current waveforms based on equivalent-time sampling.

We evaluate our progress toward the goals and milestones that were set at the beginning of the project. Our greatest success was in developing and refining the MFM/CCI technique and demonstrating its capabilities. Some of the applications that we had planned to demonstrate under this LDRD were not fully implemented because of the limitations of our system, described in this report. In a few cases (primarily for voltage imaging), the milestones were updated because of technology limitations or because of approaches developed by other workers.

We also describe the impact this project has had. Two papers on the MFM/CCI technique have been published (the first received an Outstanding Paper Award and the second was an invited paper at a European conference). A patent application has been filed on the MFM/CCI technique, one license agreement has been executed and a second is being negotiated (both involve small U. S. businesses). The MFM/CCI technology has been featured in a number of recent articles (including in Business Week and R&D Magazine). Department 2275 has an ongoing Work for Others project at the 1.0 FTE level as a direct outgrowth of this LDRD and, as a result, has been able to add 1 permanent staff member. The benefit to DOE Defense Programs is the improved IC analysis capabilities which may be applied to stockpile support and development of new DP systems.

TECHNICAL ACCOMPLISHMENTS

1. INTRODUCTION

Detailed integrated circuit (IC) analysis requires the measurement of internal conductor voltages and currents during operation. Although well-developed techniques for voltage measurement on IC conductors have been available for some time, there have been no practical techniques for determining IC currents. The ability to detect current magnitude and direction is highly desirable for design verification, analysis of analog circuits in which currents convey information, and analysis of failures whose only signature is anomalous current with no other detectable attribute. Previously, asymmetric secondary electron emission around current-carrying conductors in a scanning electron microscope (SEM) was used to detect 100 mA ac currents on IC test structures [1]. However, the utility of this approach is limited because of low sensitivity and voltage contrast effects. In the present work we describe a new technique for non-invasive imaging of currents in operating ICs based on scanning probe microscopy (SPM).

An obvious signature of charge flow in a conductor is the resulting "cylindrical" magnetic field about the conductor (Ampere's Law) [2]. Of the available techniques, magnetic force microscopy (MFM) offers the best sensitivity and spatial resolution for detection of the magnetic fields associated with currents in operating ICs. The MFM technique has been used as a sensitive probe to image magnetic fields and domains in magnetic thin films [3-6] with spatial resolution approaching 10 nm [7]. In this report we describe the first application of MFM for imaging currents in operating ICs. We demonstrate the feasibility of using the MFM current contrast imaging (MFM/CCI) technique to image currents in operating ICs and show that this technique can detect the magnitude and direction of dc current and the magnitude and phase of ac current.

The SPM can also be used for sensitive, localized detection of voltages on IC conductors by using charge force microscopy (CFM). A stated objective of our LDRD proposal was to implement CFM on our system so that both voltage and current contrast images can be obtained from a given IC sample. We implemented CFM on our Park Scientific Instruments SPM, as well as on a Digital Instruments Dimension 3000 SPM available for use near the end of this study.

An important limitation in our ability to implement this new technology in our lab was the design of the microscope itself. The SPM used for these experiments, a Park Scientific Instruments "Universal" system, is now 5-year-old technology for which non-contact mode imaging was developed but not optimized. The primary problem we encountered on our system was "tip crashes" during scanning and imaging in the non-contact mode. When the tip crashed, it came into and remained in contact with the surface, and a contact mode topology image was obtained rather than the desired MFM image. The non-contact mode, as implemented on our system, was very unstable when scanning over topography (topography of 1 μm or greater is typical for the samples used in this study). Near the end of the study, we had the opportunity to conduct a few experiments on a new Digital Instruments Dimension 3000 system that was recently obtained by Org. 1322. The

stability of non-contact mode operation is so much improved in the newer-generation SPMs that we were able to obtain MFM data from a biased IC with relatively little effort.

The characteristics of the magnetic tip are of great importance to the MFM system response. Our initial experiments were conducted with magnetic tips made by using cyanoacrylate to attach filings of a NdFeB magnet to a micromachined cantilever. These tips allowed us to demonstrate proof-of-concept of the MFM approach to detecting and imaging currents in ICs, but were difficult to produce and did not afford optimum system performance. As the study progressed, the quality of commercially available magnetic tips improved to the point that use of the commercial tips became a viable option. Experimental results obtained with tips both fabricated in our laboratory and obtained from commercial sources are presented. Fabrication of electrically conducting tips, required for CFM, is much simpler than production of magnetic thin films for MFM tips. In fact, the magnetic thin film is electrically conductive, and so in practice we used the MFM tips for CFM as well.

2. BACKGROUND: PRINCIPLES OF MAGNETIC FORCE AND CHARGE FORCE MICROSCOPY

Magnetic force microscopy is one of a growing family of SPM techniques. Samples are imaged in an SPM by scanning a sharp probe tip attached to a cantilever in close proximity to the sample surface [8,9]. There are two operating modes, contact and non-contact. MFM is a non-contact SPM technique.

In contact mode (also known as repulsive mode) SPM, the tip is brought into contact with the surface and the repulsive force between the tip and the surface is measured. As the tip is scanned across the sample, changes in this repulsive force are detected by monitoring the deflection of the cantilever. A feedback mechanism maintains this repulsive force at a constant magnitude by changing the tip-sample distance. The change in tip-sample distance is used to develop a topograpical image (strictly speaking, a constant force image) of the sample. Piezoelectric elements, capable of producing displacements as small as 0.01 nm, are used for positional control of the tip in the x, y, and z directions. Spatial resolution better than 1 nm is possible with our system.

The strong repulsive forces used for contact mode imaging are several orders of magnitude greater than the longer-range forces that are also present, such as Van der Waals, magnetic, and electrostatic forces. However, the repulsive forces fall off very quickly with distance, and become negligible when the tip is not in contact with the surface. At tip-sample separations of several nanometers to several hundred nanometers, the interaction is dominated by the longer-range forces. Operation of the SPM with these larger tip-sample separations is referred to as the non-contact mode (also known as attractive mode) [8]. Some spatial resolution is lost in the non-contact mode relative to contact mode because the tip is at a greater distance from the sample surface. Topographical images are generated primarily by tracking the Van der Waals interaction between the tip and sample. The interpretation of topographical information can be complicated by the presence of magnetic and electrostatic forces. Since Van der Waals forces (which arise from the dipole-dipole interaction between tip and sample) are relatively short-range forces

compared with the other two, the SPM signal arising from surface topography can be enhanced by placing the tip very close to the sample surface (within a few nm). On the other hand, magnetic or electrostatic information can be enhanced by moving the tip hundreds of nm away from the sample. Depending on the relative strength of the magnetic (and/or electrostatic) field and Van der Waals gradients as well as the tip-sample separation, the non-contact image may show predominantly magnetic (electrostatic) information, a superposition of magnetic (electrostatic) and topographic information, or predominantly topographic information.

The only requirement for detecting Van der Waals forces is to place the tip very close to the surface. On the other hand, in order to detect magnetic (electrostatic) fields on the sample, the tip must be magnetic (electrically conductive). Because the magnetic tips we used were also electrically conductive, it is possible to detect both electric and magnetic field gradients in the same experiment.

In non-contact mode SPM, the tip is vibrated perpendicular to the sample surface with sufficient amplitude (~ 1 nm) to prevent it from being drawn into contact with the surface by the attractive forces. Tip vibration is achieved by oscillating the cantilever supporting the tip at or near its resonant frequency. The local force gradients parallel to the direction of tip vibration (dF_Z/dz) interact with the vibrating tip and modify the effective spring constant, C, of the cantilever according to $C = C_0 + dF_Z/dz$, where C_0 is the spring constant of the isolated cantilever [8]. If the interaction is attractive, the effective spring constant C decreases, with the result that the resonant frequency also decreases. Conversely, a repulsive interaction leads to an increase in the resonant frequency. In addition to changes in the resonant frequency, the local force gradient also modifies the amplitude and phase of the cantilever's vibration at resonance. By monitoring changes in frequency, phase, or amplitude of the cantilever's vibration, the local force gradient can be measured.

3. EXPERIMENTAL APPROACH

3.1 Simulation of MFM/Current Contrast Imaging

A simple computer model was developed to assess the feasibility of using MFM to image current in operating ICs. The model was used to calculate the magnetic fields produced by different currents in several parallel, straight conductors and to simulate the MFM image for the given conditions. The conductors were assumed to be infinitely thin, infinitely long, and spaced 5 μm apart. The local magnetization was assumed to be zero (0) and the permeability of free space was used for all modeling. The magnetic field around the four parallel conductors in the model is the superposition of the fields generated around each one.

Figure 1 shows a cross-section through the conductors and indicates the magnitude and direction of the dc current through each. The background contrast indicates the vertical component of the magnetic field, H_Z, above the conductors. As discussed in the Section 2, H_Z is the component of the magnetic field to which the MFM is most sensitive. Figure 2 is a linescan showing the variation of H_Z with position (x) at a height of 1 μm above the

conductors. Because of the passivation layer on ICs, the MFM tip will typically be at least 1 μm above the conductors. The model does not include an attenuation factor for the passivation because it does not appreciably reduce the magnetic field intensity. The magnetic field strengths are on the order of microtesla (μT) for the simulated currents. Figure 3 shows the simulated MFM image of an isolated, straight conductor with 2 mA dc current. Beginning at the bottom of the figure, the dc current was initially - 2 mA. The bright-to-dark transition (from left to right) occurs because H_z changes sign above the conductors as indicated in the linescan shown in Figure 2. The y-axis in Figure 3 indicates both distance along the conductor and time of the raster scan. When the current direction was reversed (e.g., from -2 mA to + 2 mA as indicated in Figure 3), the bright-to-dark contrast in the simulated image was also reversed.

Three-dimensional simulations using actual IC conductor geometries have been performed [10,11] based on the theory of Hartmann [12]. Our results are in good agreement with those of the 3-dimensional models at a distance of 1 μm (passivation thickness) from the conductor.

3.2 Experimental Implementation of MFM and CFM for Current Contrast and Voltage Contrast Imaging

3.2.1 Non-Contact Mode Imaging. A Park Scientific Instruments SFM-BD2 "Universal" System scanning probe microscope with a non-contact mode detection module was used to acquire MFM data and images. For image acquisition, the frequency modulation (FM) non-contact mode was employed. The system first determines the resonant frequency of the freely-vibrating cantilever (i.e., with no forces acting on it). A "set point" operating frequency is selected away from (below) the resonant frequency by an amount proportional to the desired interaction force between the tip and sample. During imaging, the vibration amplitude of the cantilever is held constant and a feedback circuit adjusts the tip-sample separation to maintain a constant force gradient corresponding to the set value. The amount of tip displacement in the z direction to maintain a constant force gradient is used to map out a force gradient image.

We had difficulty with tip crashes in the experiments carried out using the Park Scientific Instruments "Universal" system in the non-contact mode. However, tip crashes were minimized by driving the cantilever and feeding back on the third harmonic of the cantilever's vibrational response ($3\omega_0$) rather than the first harmonic (ω_0) as is usual. In addition to minimizing tip crashes, operating at $3\omega_0$ was necessary because the attached magnet reduced the natural frequency of the cantilever so much that ω_0 is out of the operating range of the non-contact module. Successful operation at $3\omega_0$ was achieved by increasing both the gain and the time contstant relative to operating at ω_0.

3.2.2 Magnetic and Conductive Tips. The characteristics of the magnetic tip are of great importance to the system response. It is noted that there are important differences between the sensors required for MFM imaging of magnetic recording media and those needed for MFM/CCI. A tip with a relatively weak magnetic dipole moment is required for imaging recording media because a strong magnetic sensor could distort the data being acquired

[13]. Tips with a relatively weak magnetic dipole moment are sufficient for imaging magnetic media and magnetic recording heads because the fields being sensed are relatively strong. In MFM/CCI of ICs, the magnetic fields are weaker and a sensor with a stronger magnetic dipole moment is required. The use of a strongly magnetized tip does not present a problem with respect to distorting the data because the sample has no permanent magnetic properties which could be altered by magnetic fields from the sensor.

3.2.2.1 Magnetic Tips Fabricated at Sandia. Our initial results were obtained with magnetic tips that were fabricated by attaching small (approximately 20 - 50 μm) particles, filings from a commercially-available rare earth (NdFeB) permanent magnet, to micromachined Si_3N_4 cantilevers. Figure 4a shows a micromachined cantilever with an integrated pyramidal tip and Figure 4b shows such a cantilever with a magnetic particle attached. A cyanoacrylate material was used to attach the magnetic filings to the cantilevers. A microprobe station was used to place cyanoacrylate and a magnetic filing on each cantilever. While this approach yields tips with sufficient magnetic dipole moment to detect and image currents in operating ICs, there are several limitations. First, for ease of data interpretation, it is preferable to use tips with the magnetic dipole moment oriented normal to the surface. Second, the geometry of the tips was not well-controlled. Some of the tips (including the one shown in Figure 4b) were relatively large, irregular in shape, and fairly blunt, which reduced the spatial resolution of the technique. Third, it is desirable for the magnetic tips to be readily manufacturable and to have reproducible magnetic properties. Our fabrication technique fulfilled none of these requirements, but was sufficient to demonstrate proof-of-concept.

3.2.2.2 Thin Film Magnetic Tips. During the course of this study, magnetic tips suitable for magnetic current contrast imaging became commercially available from a few sources. We found the tips available from Digital Instruments to be the most useful. Those sensors are micromachined silicon force sensors which are sputter-coated on the "tip" side with several hundred Å of a Co-Cr alloy. The domains in the magnetic thin film are aligned with a strong permanent magnet prior to installing the tip in the SPM. We found that the current sensitivity with the thin film tips was a factor of 20 - 40 lower than with the handmade tips, but that the spatial resolution was dramatically increased to well into the submicron range. The experiments conducted with the thin film tips are discussed in greater detail in Section 4.5.

We also conducted experiments using tips where a solenoid winding had been placed around the base of the cantilever, as shown schematically in Figure 5. A current passed through the windings served to remagnetize the tip. We found that the thin-film magnetic tips needed to be magnetized with a strong permanent magnet prior to use (otherwise, passing a current through the solenoid windings has no effect). The degree to which the tips can be remagnetized was found to vary from tip to tip. The experimental results are described in Section 4.5.

3.2.2.3 Electrically Conductive Tips. Early experiments were conducted with silicon nitride cantilevers sputter coated with a Au-Pd alloy. Most experiments employed the Digital Instruments MFM tips, coated with a conductive Co-Cr alloy. In addition, we obtained a modified Park Scientific Instruments AFM head to permit application of an external voltage to the cantilever (in the original design, the cantilever was tied to ground

potential). This modification permits both static and a time-varying signals to be applied to the tip.

3.2.3 DC and AC Stimulation. MFM current contrast images were obtained with both dc and ac stimulus. DC stimulus gives rise to static magnetic fields around the conductor, which are readily detected by attractive mode imaging. It is also possible to detect ac currents by taking advantage of the mechanics of the vibrating cantilever, which can be represented as a simple harmonic oscillator. When ac stimulus is applied to an IC, the magnetic field and field gradients vary with the frequency of the applied signal, ω_1. The vibration amplitude, A, of a simple harmonic oscillator with applied external force can be expressed as $A \propto 1/(\omega_0^2 - \omega_1^2)$ where ω_0 is the resonant frequency [14]. As the ω_1 approaches ω_0, the amplitude of vibration increases rapidly. In practice, this means that the sensitivity of the system increases dramatically if the ac signal is applied to the conductor at ω_0.

In general, ICs are powered with dc levels (e.g., 3.3 or 5V dc). However, it is still possible to take advantage of the increased detection sensitivity that occurs with ac stimulation by operating with a small ac voltage ripple (millivolts) on the dc power supply or by clocking (operating) the IC at ω_0. An example of the ac ripple approach is given in Section 4.4.

CFM imaging was also performed with both dc and ac stimulus. The procedures for CFM detection are similar to those used for MFM imaging. Instead of passing a current through the conductor, a voltage is maintained between the tip and conductor. As was the case for MFM, a marked enhancement in sensitivity (for CFM, two orders of magnitude) was observed if the ac signal is applied to the conductor at the cantilever resonant frequency.

3.2.4 MFM and CFM Signal Acquisition. A schematic of the acquisition system used in our experiments is shown in Figure 6. The main console controls the fine mechanical approach, the piezoelectric scanning (x, y, and z) of the sample and the piezoelectric element that vibrates the cantilever at resonance, which is referred to as a bimorph. The console also contains a frequency detection circuit that has a range between 60 kHz and 270 kHz (refer to Section 3.2.1). Because of the relatively large tip mass, the cantilevers illustrated in Figure 4b have a very low resonant frequency, typically 22 kHz. The system is capable of sensing harmonics of the resonant frequency, and a reference frequency of ~66 kHz was selected. As described in Section 3.2.1, operating at $3\omega_0$ minimized tip crashing.

Electrical stimulation was performed with both dc and ac current. A variable resistance switch box was used to select the ac current through the IC. The cantilever's resonance signal (the output from the position sensitive photodetector) was used to trigger a function generator to insure synchronization with the cantilever's resonant frequency during ac experiments. Because the sample stage rather than the tip is scanned in our system, it was necessary to avoid restricting the motion of the sample stage with multiple electrical connections from the bias source to the sample. Our approach was to connect only two conductors to the IC package on the SPM stage. Electrical connection was made from these two pins to all the necessary pins on the IC by wire bonding.

In order to use the SPM to image an IC, the tip must be brought into close proximity with the die surface. In SPM jargon, this procedure is referred to as "tip approach", or "approaching the tip to the sample". Approaching the tip to the surface of a packaged IC was at times a difficult mechanical problem due to the design of the microscope. Figure 7 is a schematic representation of an SPM test head and a packaged IC. Packaged ICs are much smaller, relative to the size of the SPM head, than is shown in Figure 7. The figure shows that the package well (the cavity in which the IC is mounted) can be fairly deep. In addition, the hardware which supports the cantilever is fairly wide. As a result, problems were encountered approaching the tip to the sample when the package well was small (preventing the cantilever tip from reaching the sample surface) or if we desired to image the area of the chip near the edge of the package well. It is noted that SPMs were originally designed to examine small, flat samples. In the time since our instrument was purchased, SPM manufacturers have made great strides in increasing the flexibility of their sample platforms. A good example of this is the development of large mechanical translation stages that permit the examination of any point on a silicon wafer for metrology applications. Such a platform could be adapted to accommodate larger IC packages and possibly even the fixtures required to fully bias an IC during SPM examination. However, the approach of an SPM tip into a packaged IC will still be an issue, because the cantilevers are generally mounted on a support that is fairly wide. As IC analysis applications of the SPM have become more well known, the SPM manufacturers have become more receptive to the idea of devising solutions to enable packaged ICs to be easily examined.

As the force on the tip changes, the cantilever is deflected. The cantilever position is detected by reflecting a laser beam off the back of the cantilever, and observing the change in position at a position-sensitive photodetector. The coarse tip positioning is performed by mechanically lowering the SPM test head into the package well, and the fine approach of the tip to the sample is computer-controlled. Note that the SPM test head must be at an angle to clear the sides of the IC package cavity. Figure 8 is a schematic high magnification view of a cantilever with a magnetic tip attached in close proximity to the sample. The micromachined cantilever and its tip are much smaller than the Pyrex base attached to the SPM test head.

4. MFM IMAGING AND MEASUREMENT RESULTS

4.1 DC Analysis

Figure 9 is an optical micrograph of the test structure used for dc and ac current imaging analysis. The two aluminum conductors shown are each 4 μm wide. Current is passed through the conductor on the right. The conductor on the left is electrically floating for all measurements and imaging. For optimal signal and spatial resolution, the gain of the z-piezoelectric drive was maximized and the scan speed minimized. The high gain of the z-piezoelectric feedback maximized the SPM's response (and hence signal) to the forces encountered while scanning. The slow scan speed (15 minutes/image) ensured that the SPM could respond to magnetic forces encountered during the raster scan before the cantilever had moved away from the source of those forces. The slow scan speed also minimized the tip crashing problem previously mentioned in Section 3.2.1.

Figure 10 is an MFM image of the passivated test structure shown in Figure 9 with ± 2 mA dc current in the conductor. The current was initially - 2 mA, and the corresponding MFM image is the bottom third of Figure 10. The current direction was reversed during acquisition of the image. The middle section of the image displays the vertical magnetic field gradients when the applied current is + 2 mA, and at the top of the image the current is again - 2 mA. The conductor is located at the bright/dark-dark/bright interface in the middle of the image. Note the similarity between Figure 10 and to the simulated MFM image shown in Figure 3.

Images similar to Figure 10 were also obtained for applied dc currents of ± 500 μA and ± 250 μA. As indicated in Section 3.2.3, the MFM signal decreases as the applied current drops. For applied dc currents of < ± 250 μA, the signal was lost in the noise for the particular tip used to obtain these images.

4.2 AC Analysis

AC square wave currents were also analyzed using the test structure shown in Figure 9. As discussed in Section 3.2.3, large increases in current (magnetic field) sensitivity can be achieved by changing the current through the conductor at the resonant frequency of the cantilever. Experimentally this was accomplished by using the output of the position-sensitive photo detector to trigger a function generator used to produce the ac square wave applied to the conductor. Figure 11 shows the MFM signal of a 20 μA peak-to-peak current through the conductor. Halfway through acquisition of the image the phase of the ac current was changed by 180^0, causing the bright/dark signal to shift sides of the conductor. (This is similar to the effect caused by reversing the current direction in dc stressing). The increase in sensitivity with ac current was so great that smaller magnetic tips with a reduced net magnetic dipole moment (not usable for dc measurement) were adequate for ac analysis. The use of a physically smaller tip both increased the spatial resolution and allowed the tip to be placed close enough to the sample that the topology of the unbiased conductor on the left is now visible as a Van der Waals force image superimposed on the magnetic field image.

We observed two major limitations when obtaining ac current contrast images. The first is that we had greatly increased sensitivity - so much so that the tip sometimes needed to be moved further from the surface than for dc imaging to prevent tip crashing (an example of this is given in Section 4.4). The second difficulty is that the current range in which we could obtain current contrast images was small: we could see differences between 2 and 20 μA ac, but we could not tell the difference between 20 μA and 1 mA ac, they both saturated the response of the SPM system. Both of these problems could be alleviated by a more flexible system configuration that would allow the detection sensitivity to be varied to suit the particular application. A straightforward way to achieve this is to vary the phase between the photodetector signal and the ac current applied to the sample to minimize or maximize the harmonic force. The function generator used for these experiments did not permit the phase to be varied between the source (photodetector signal) and the generated signal.

4.3 Current Sensitivity of MFM/CCI

By "parking" the MFM cantilever close (~10 μm) to one side of the conductor and monitoring the change in MFM signal with applied current, the sensitivity of the MFM to differences in applied current can be demonstrated. Figure 12 shows a plot of normalized MFM signal response to applied dc current. Zero (0) MFM signal at zero (0) current has been added as a data point in Figure 12 with no error bars. These data indicate that a change of ~ 1 mA over the ± 5 mA range is easily detected. A "best-fit", 3rd order polynomial fit to the data is displayed in Figure 12. The exact shape of the curve depends upon the effect of external force gradients on the cantilever's resonance properties as well as the MFM system's response over the signal range.

Figure 13 shows the MFM signal response to ac currents. These data were also acquired by "parking" the cantilever and acquiring the MFM response versus applied ac current. The straight line fit of the data in Figure 13 indicates that shifts of ~1 μA can be detected over this 20 μA peak-to-peak ac range.

Note that Figures 12 and 13 *do not* indicate that currents can arbitrarily be measured to within 1 mA dc or 1 μA ac, but *do show* that *changes* in current magnitude as low as 1 mA dc and 1 μA peak-to-peak ac can be detected. The lateral "parking" distance from the conductor, the vertical distance above the surface of the IC, the set point frequency, and the particular cantilever used all contribute to the MFM's response to different currents (magnetic fields). Further work to standardize these variables will be necessary to make accurate, quantitative current measurements.

When measurements were made with the tip "parked", the track function on the SPM was switched to the "hold" mode. In the "track" mode, the system senses relative differences in signal as the image as scanned, which helps compensate for system drift but overlooks dc forces. However, if the tip is parked, only the initial change in force (e.g., when the current was switched from one level to another) would cause a signal in the track mode. In the "hold" mode, dc forces produce a constant change, and so we used that mode.

4.4 Application of MFM/CCI to a Defective IC

A damaged IC with elevated power supply current was examined with MFM/CCI. The IC has two levels of metal interconnect (1.25 μm wide metal-1 and 1.75 μm wide metal-2). A metal-1 to metal-2 short was produced by using a laser to fuse a metal-2 signal conductor to a metal-1 V_{DD} power bus. The IC drew 10 mA dc current with 3.3 V applied bias. Most of this current results from the metal-1 to metal-2 short since the IC current level was < 50 μA at 5 V before laser fusing.

Figure 14 is a dc MFM/CCI image of the elevated current path on the damaged IC. The bright/dark interface that runs horizontally from the lower left to center and then vertically indicates the conductor location. Figure 15 is an optical micrograph of approximately the same field of view as Figure 14, with the current-carrying conductors highlighted in white. Even though the current path is "L"-shaped as shown in Figures 14 and 15, the conductor actually has a "T" shape, with the conductor forming the vertical part of the current path running from the top to the bottom of the image. Electrical continuity was confirmed at this interconnection by using voltage contrast imaging, a scanning electron microscopy

technique used for imaging voltages on IC conductors. This demonstrates that the actual current path can be determined by MFM/CCI from among multiple possible paths, and that the previously-developed voltage contrast imaging techniques cannot provide this information.

The same IC was also examined using ac current (Figure 16) with results similar to those obtained for the dc case. The IC was supplied with a dc voltage of 3.225 with a superimposed ac ripple of 0.075 V. This concept of applying a "ripple" to the IC's power supply has been introduced for I_{DDQ} testing with no adverse effects on the IC [15,16]. It may be noted that the image in Figure 16 is not as crisp as that in Figure 14, reflecting a loss in spatial resolution. This arose because of the large increase in sensitivity when operating in the ac mode. The increase in cantilever response led to increased problems with tip crashing. The tip had to be moved farther from the sample to achieve stable cantilever vibration without crashing, and as a result the spatial resolution was degraded.

The dc and ac MFM/CCI images shown in Figures 10, 11, and 14 were obtained from passivated structures. However, no differences in spatial or current resolution were observed with the passivation removed. This is probably a result of the large size of the magnetic tip used compared to the passivation thickness combined with a relatively large tip - sample distance in our experiments. It is also noted from Figures 14 - 16 that overlying metal-2 does not obscure the MFM signal from current in a metal-1 line.

4.5 MFM and CFM Experiments with Thin Film Coated Tips

4.5.1 Tips Coated with Magnetic Thin Films. We have used micromachined cantilevers which are sputter-coated on the "tip" side with several hundred Angstroms of a Co-Cr alloy for both MFM and CFM measurements. We conducted experiments with both a Park Scientific Instruments "Universal" system and a Digital Instruments Dimension 3000 system. In MFM, the tip was first magnetized with a permanent magnet. To determine the sensitivities for both dc- and ac- current detection, we parked the tip hundreds of nm directly above an IC conductor (such as the one shown in Figure 9) and monitored the observable changes in the resonant frequency of the cantilever as the currents in the conductor were varied. For MFM, the dc and ac sensitivities were determined to be ~ 20 mA and 40 μA (peak-to-peak), respectively. These are a factor of 20 and 40, respectively, less sensitive than were obtained with the tips fabricating by gluing a NdFeB magnetic particle to a cantilever. However, the spatial resolution is considerably improved. The ac enhancement is achieved by applying current to the conductor at the resonant frequency of the cantilever as described in Section 4.2. The procedures for CFM measurements are quite similar to those for MFM, except that a voltage is applied between the tip and the conductor. The dc and ac sensitivities are determined to be ~ 500 mV and 10 mV (peak-to-peak) respectively.

We have also used the thin-film tips to investigate both the magnetic force gradient and magnetic force profiles across a conductor. The magnetic force gradients were measured by detecting changes in resonant frequency of the cantilever as described in detail in Section 3.2.1. Figure 17, for example, shows a magnetic force gradient profile across an 8 μm wide conductor with a dc current of 100 mA. The tip-sample separation was

maintained at ~ 300 nm during the scanning. To better understand the force gradient profiles, we performed numerical simulations of the magnetic force gradient by allowing the tip dipole moment orientations to vary from parallel ($\theta = 0^0$) to perpendicular ($\theta = 90^0$) to the surface normal (Figure 18). The experimental force-gradient profiles, however, do not match exactly any of the simulated profiles, suggesting that the magnetic dipole moments are generally not parallel to the surface normal and are not aligned uniformly across the tips.

The experimental setup for measuring the magnetic-force profiles, shown in Figure 19, is different from that for measuring magnetic-force-gradient profiles. A sinusoidal ac current (500 mA peak-to-peak) at the resonance frequency of the cantilever (ω_0) was applied to an 8 μm wide conducting line. The magnetic force between the tip and sample caused the cantilever to vibrate at ω_0. The vibration was monitored with a position-sensitive photodetector whose output was fed into a lock-in amplifier tuned to ω_0. The output of the lock-in amplifier was stored in the computer via an analog to digital conversion board. During the scanning, the tip-sample separation was maintained at ~ 3 μm. Figure 20a, for example, shows an experimental magnetic-force profile. Numerical simulations were also performed and it was found that the experimental profile corresponded best to the simulation that assumed the orientation of the average magnetic dipole moments to be 25^0 from the surface normal (Figure 20b). Nevertheless, the experimental curve still does not exactly match the simulated one, suggesting once again that the magnetization may not be uniform across the tip.

4.5.2 Enhanced Magnetic Thin Film Tips. We conducted experiments using tips where a solenoid winding had been placed around the base of the cantilever (Figure 5). A current passed through the windings served to produce a static (with a dc current) or time-varying modulation (with an ac current) of the tip magnetic dipole moment. A current amplitude of 100 mA to 1.0 A was needed to enhance the tip magnetization ("remagnetize" the tips). No change in magnetic dipole moment was observed unless the tip had been first magnetized with a strong permanent magnet. It was also found that the degree to which the magnetic dipole moment could be changed varied from tip to tip.

The effect of a dc current on the tip magnetic dipole moment is demonstrated by imaging a magnetic disk before and after remagnetization of the tip. We typically use a sample of magentic disk or tape to check a tip's performance prior to using it for MFM/CCI. Figure 21 shows an image of a magnetic disk for a weakly magnetized tip. The image was taken in non-contact mode with tip-sample separation of ~10 nm. The image consists mainly of topographic information with a series of very weak magnetic stripes (as indicated by the arrow). The magnetic information disappeared if the tip was further separated from the sample. Figure 22 shows an image after the tip was remagnetized with a 200 mA dc current for 5 minutes. Even at a tip-sample separation of 500 nm, the magnetic stripes are clearly visible.

The effect of ac modulation is demonstrated by monitoring changes in magnetic force between a modulated tip and a conductor. The experimental setup for this measurement is similar to that for measuring magnetic-force profiles (Figure 19). Instead of scanning the tip across the conductor line, we parked the tip directly above this line while passing 100 Hz ac

currents through the solenoid. In addition, the output of the lock-in amplifier was connected to an oscilloscope for display instead of to a computer for storage. Figure 23 shows the waveforms displayed on the oscilloscope. These waveforms have the same characteristics as the current waveforms passing through the solenoid. For example, a triangular waveform was observed on the oscilloscope as we applied a triangular-wave current through the solenoid. These results confirm that ac modulation indeed takes place at the tip. The effect of ac modulation at the tip is, however, relatively small. In order to obtain an observable signal, large currents (0.5-1.0 A peak to peak) had to be applied at both the conducting line and the solenoid.

4.6 Large Area Scanning

An important limitation of MFM/CCI based on a standard SPM is that the largest scan area is approximately 250 μm x 250 μm, and such a scan takes several minutes to set up and execute. Clearly, to image an entire IC (tens of square millimeters) will take a prohibitively long time (weeks), require a huge amount of disk storage space (hundreds of megabytes), and provide a tremendous amount of extraneous information. A failure analysis application we anticipate is to scan an entire IC quickly to localize the elevated current paths.

We performed an experiment in which a Newport precision mechanical translation stage rather than the x and y piezoelectric scanners to translate the sample in the x- and y-directions. The force detection electronics on the SPM were used to detect the interaction between the magnetic tip and the magnetic field due to a 20 mA ac current in the test structure (again, the 4 μm wide x 1 μm thick aluminum metallization line). Such a large current was used because the tip was far (~1 mm) from the sample. We scanned an area approximately 600 μm x 220 μm. While this stage was very precise (25 nm resolution in x- and y-directions), it was also very slow. Thus, to expedite imaging the sample, we used a relatively large pixel size (10 μm x 10 μm). Clearly, in a dedicated system for quick diagnostic scanning of an IC, a lower spatial resolution could be tolerated to obtain faster imaging. The image obtained from this experiment is shown in Figure 24.

We did not attempt to scan a larger area because the test chip was not level in the x-y plane in our crude setup. Thus, the distance between the tip and sample varied over the scan area, and the amount of variation would further increase with increased scan area. The variation in tip height leads to the problems of crashing the tip into the sample during the portions of the scan when the tip is closer to the sample, obtaining a weak SPM signal when the tip is far from the surface, and obtaining a non-uniform response to a given current over the scanned area.

This experiment has demonstrated the proof-of-concept; a more sophisticated fixturing system could be devised to allow the tip to be scanned over large samples at a constant height to a reference plane. We elected not to pursue further developments of large area scanning under this project because (1) it was perceived that placing our emphasis on tip development and implementing CFM had greater impact, and (2) SPMs with integrated scanning stages, which could be used for large area scanning, are becoming increasingly available commercially.

4.7 Current Waveform Acquisition

Voltage waveform measurements using SPM at high frequencies (GHz) have recently been performed at Stanford University using equivalent-time sampling [17]. This equivalent-time method can analogously be applied for current waveform measurements. The prerequisite for this type of measurement is the ability to modulate the magnetic dipole moment of the tips which we have clearly demonstrated in the low-frequency ac modulation experiments. The question remains whether this type of thin film coated tip can respond to high-frequency modulations. Other potential limitations associated with thin-film tips for quantitative current waveform measurements include lack of sensitivity (due to the weak modulation effect), uncertainty in the tip dipole-moment orientation and non-uniformity of the tip magnetization. There is definitely a need for development of a magnetic sensor with well-characterized, reproducible magnetization. A potential solution that we are actively exploring (beyond the scope of this LDRD) is a micromachined inductor-coil type sensor.

5. DISCUSSION

The major limitations that we encountered in this study had to do with the SPM platform that was used for our experiments. The first limitation was presented by the system design. SPMs were originally designed for examining small, flat samples. In our system, performing imaging on packaged ICs is complicated by the relatively small area (less than 1" x 1") into which the sample is placed. Adding a fixture to provide electrical stimulus to the package pins was not possible. For our experiments, we were able to apply power to the IC by attaching leads directly to several of the package pins. For static biasing, we used internal wire bonding to connect together package pins that were driven to the same potential in order to minimize the number of external wires attached to the IC package. The other system design problem described in this report is that the hardware that holds the cantilever makes it difficult to place the tip into a small IC package or to image the edge of an IC near the package well.

The second limitation was tip crashes during non-contact mode imaging. This severely limited the utility of our SPM system for scanning and imaging. As a result, we did not use our MFM/CCI system to characterize as many real IC failures as we had intended in our original project plan. The tip was much less likely to crash in system when we "parked" the tip, and that approach was used to a large extent in our characterization of thin film coated tips.

These limitations are for the most part engineering problems, not fundamental technological problems, and can be overcome by an SPM design specifically for implementing MFM and CFM analysis on packaged ICs or wafers. In fact, the problem of instability in the non-contact mode seems to have been addressed already by at least one SPM manufacturer. The experiments we performed with the new Digital Instruments SPM (which uses "Lift Mode" to first perform a contact mode image to find the sample surface and then raises the tip to a user-selected distance above the sample surface to collect the non-contact mode image) exhibiteded substantially reduced tip crashing. The major SPM vendors now supply large area mechanical translation stages that, while designed for wafers, could also accommodate large IC packages and fixtures.

6. CONCLUSIONS

We have demonstrated the ability to image internal IC currents non-invasively for the first time. The magnetic fields associated with current-carrying conductors were imaged by the MFM/CCI technique. The MFM/CCI technique has demonstrated sensitivities of 1 mA dc and 1 μA ac, and is an important new capability for failure analysis, design verification, and model validation. These results indicate the great potential of applying MFM to IC failure analysis and the growing importance of scanning probe microscopy in microelectronics.

We have also implemented CFM, permitting voltages on IC conductors to be detected with a sensitivity of 500 mV dc and 10 mV ac. Both current and voltage imaging of internal conductors on operating ICs are now feasible by combining the MFM and CFM techniques demonstrated here. We have also demonstrated an approach that will permit relatively rapid imaging of an entire IC in order to localize the elevated current paths on a failing device. In addition, we described an approach that can be used to obtain current waveforms. The combination of all these features in a system engineered specifically for examining ICs will be a powerful new IC analysis tool.

7. ACKNOWLEDGMENTS

The authors thank the Sandia National Laboratories LDRD Program office for support of this work. We also thank Jack Houston (Sandia Org. 1114) for helpful discussions, Arnold Howard and Leo Griego (Sandia Org. 1322) for the use of and assitance with their Digital Instruments Dimension 3000 system, Meliton Gonzales (Sandia Org. 2412-1) for placing the windings on the base of the MFM sensors, and Ken Peterson and Bill Curtis (Sandia Org. 2275) for their careful review of the manuscript.

8. REFERENCES

1. K. Helmreich, P. Nagel, W. Wolz, K. D. Muller-Glaser, Proceedings of the International Test Conference (1991) 256.
2. D. Halliday and R. Resnick, Physics, John Wiley & Sons, Inc., New York, 844 - 846, 1966.
3. Y. Martin and H. K. Wickramasinghe, Appl. Phys. Lett., 50 (1987) 1455.
4. Y. Martin, D. Rugar, and H. K. Wickramasinghe, Appl. Phys. Lett., 52 (1988) 244.
5. H. J. Mamin, D. Rugar, J. E. Stern, B. D. Terris, and S. E. Lambert, Appl. Phys. Lett., 53 (1988) 1563.
6. P. C. D. Hobbs, D. W. Abraham, and H. K. Wickramasinghe, Appl. Phys. Lett., 55 (1989) 2357.
7. P. Grutter, Th. Jung, H. Heinzelmann, A. Wadas, E. Meyer, H.-R. Hidber, and H.-J. Guntherodt, J. .Appl. Phys., 67 (1990) 1437.
8. D. Rugar and P. Hansma, Physics Today, (October 1990) 23.
9. H. K. Wickramasinghe, Scientific American, (October 1989) 98.
10. R. Proksch, unpublished results.
11. T. Goddenhenreich, H. Lemke, M. Muck, U. Hartmann, and C. Heiden, Appl. Phys. Lett., 57 (1990) 2612.
12. U. Hartmann, J. Vac. Sci. .Technol. A, 8 (1990) 411.
13. P. Grutter, D. Rugar, H. J. Mamin, G. Castillo, S. E. Lambert, C.-J. Lin, R. M. Valletta, O. Wolter, T. Bayer, and J. Greschner, Appl. Phys. Lett., 57 (1990) 1820.
14. H. Goldstein, Classical Mechanics, 2nd ed., Addison-Wesley, Reading, MA, 264 - 265, 1980.
15. M. W. Levi, Proceedings of the IEEE Test Conference, (1981) 217.
16. J. M. Soden, C. F. Hawkins, R. K. Gulati, and W. Mao, J. of Electronic Testing, 3 (1992) 291.
17. A. S. Hou, F. Ho, and D. M. Bloom, Electronics Letters, 28, (1992) 2302.

9. FIGURES

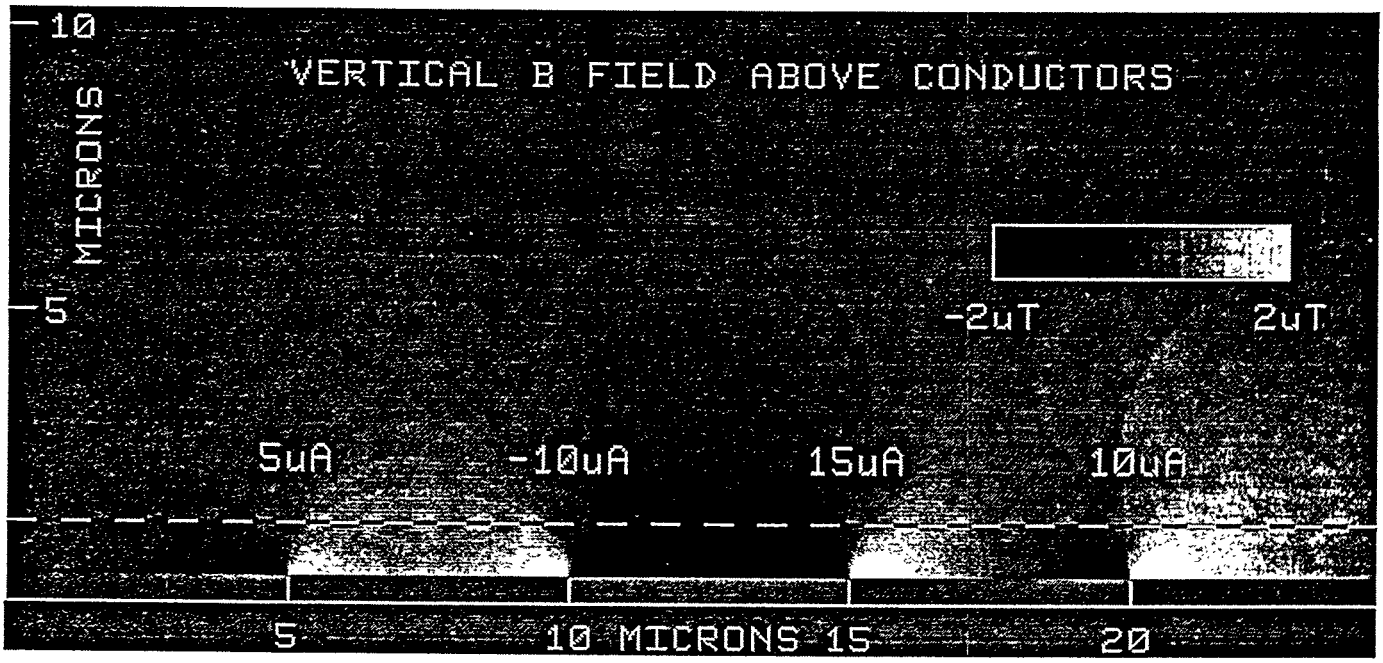

Figure 1. Simulation of vertical magnetic field component, H_z, above four parallel current-carrying conductors.

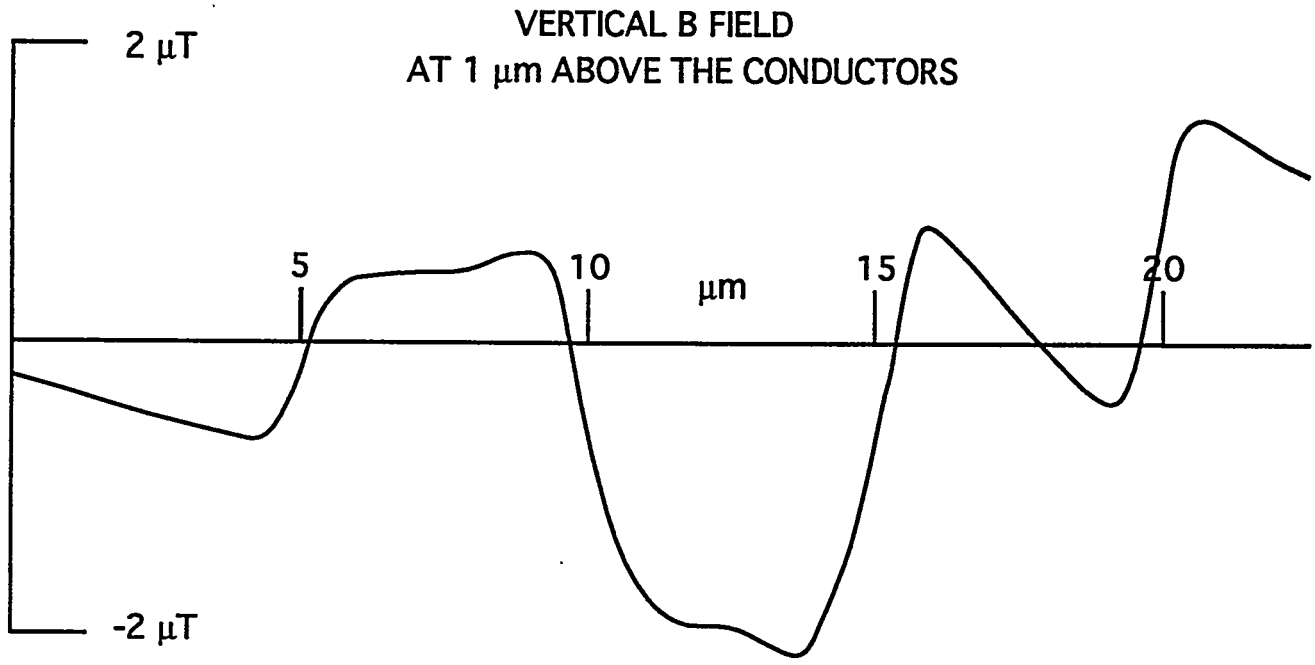

Figure 2. Simulation of an MFM linescan 1 μm above the conductors shown in Fig. 1.

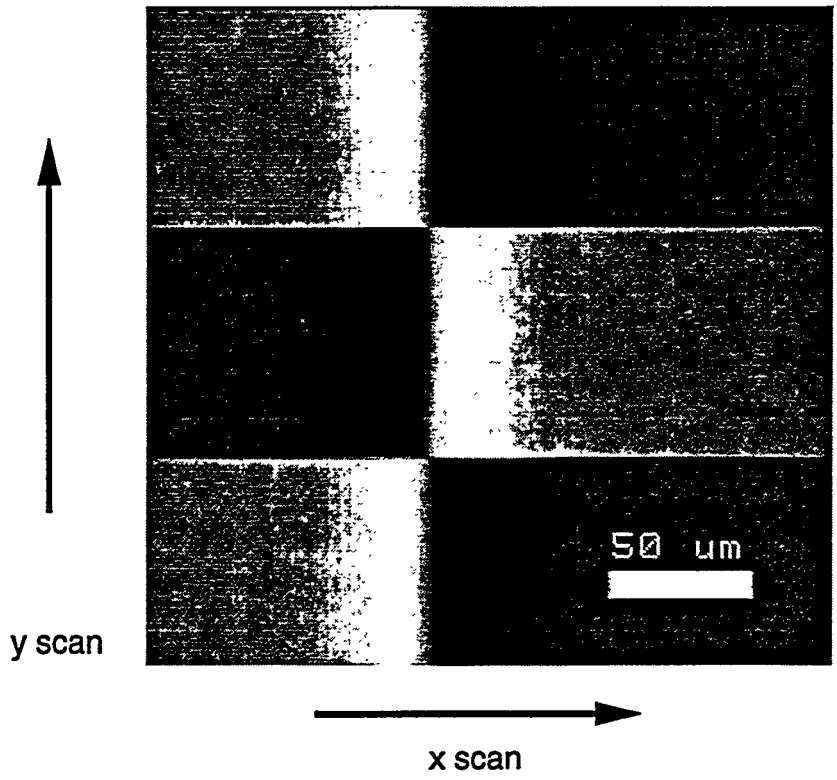

Figure 3. Simulated MFM image of a conductor carrying 2 mA dc current.

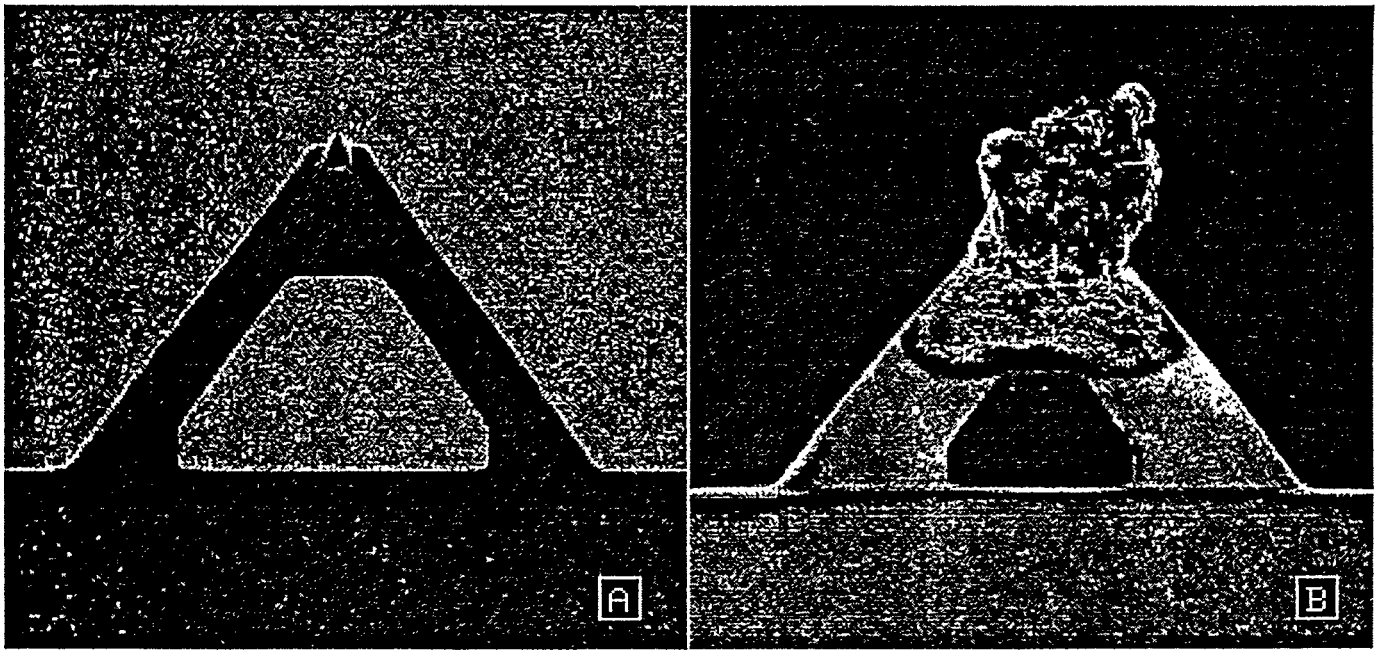

Figure 4. (a) SEM image of a micromachined Si_3N_4 cantilever with integrated pyramidal tip. The tip is approximately 4 μm across at its base. (b) MFM tip fabricated by attaching a NdFeB filing to a micromachined Si_3N_4 cantilever.

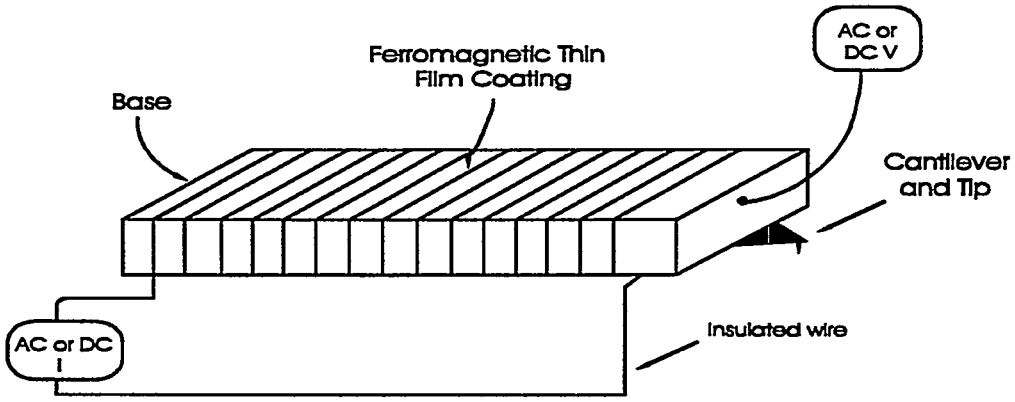

Figure 5. Schematic representation of a micromachined cantilever with a solenoid winding around the base.

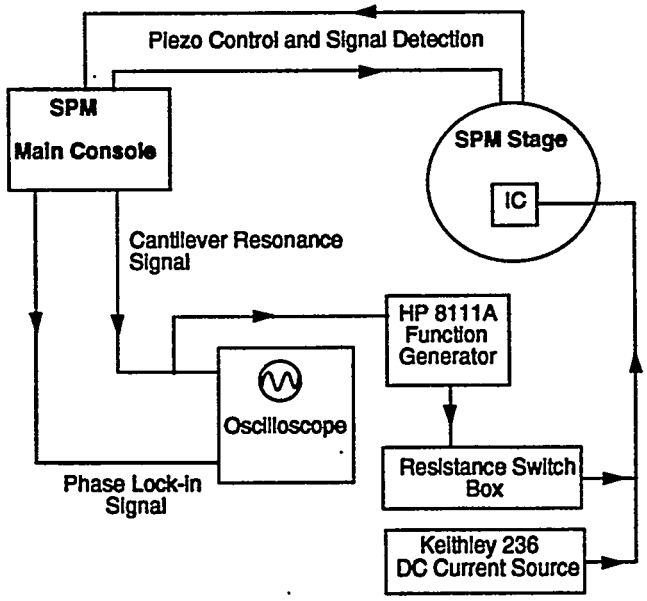

Figure 6. Schematic of the MFM acquisition system.

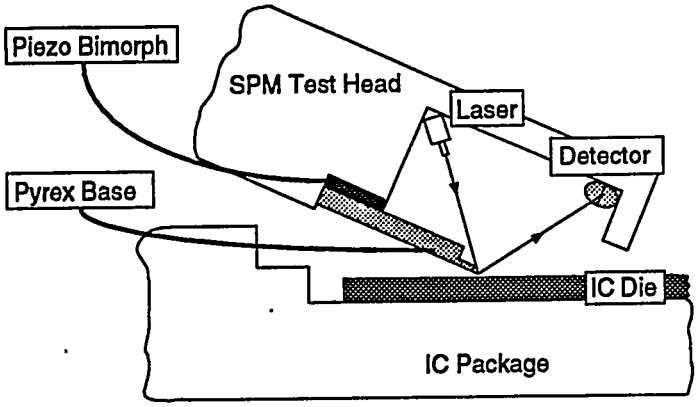

Figure 7. The SPM test head in position to acquire data from a packaged IC.

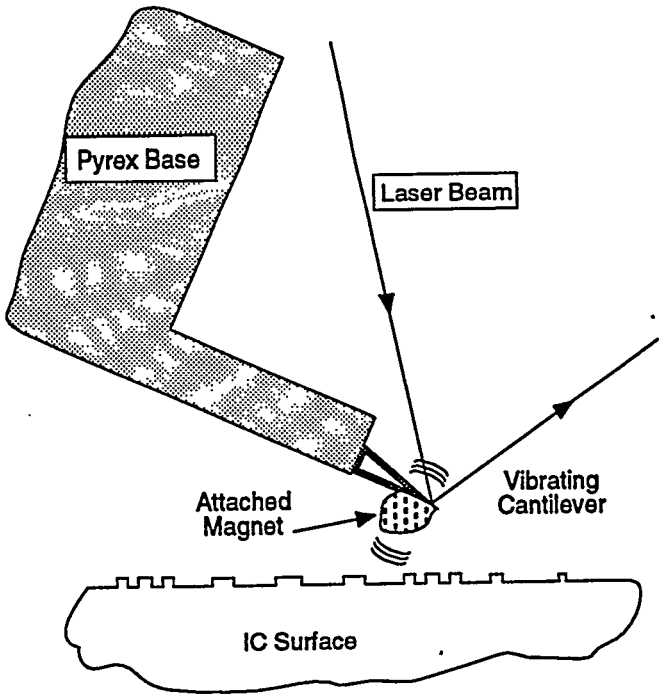

Figure 8. The vibrating cantilever interacts with fields near the IC surface.

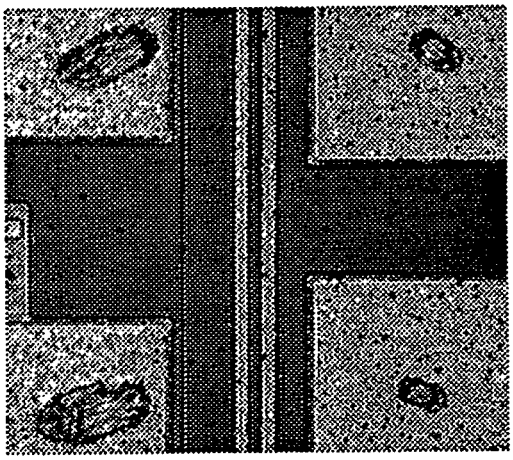

Figure 9. Optical micrograph of passivated test structure used for dc and ac analysis. The two conductors run vertically between the four bond pads.

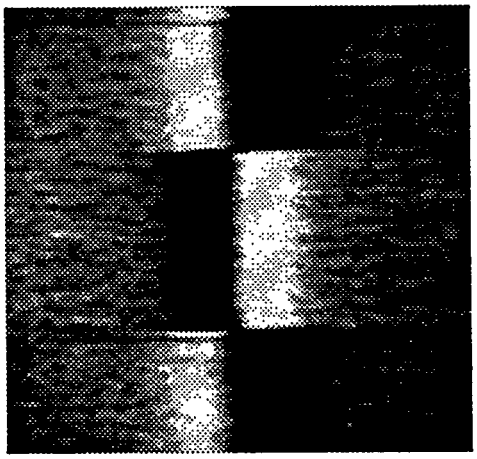

Figure 10. MFM image of the test structure in Figure 9 with ± 2 mA dc current applied during the raster scan.

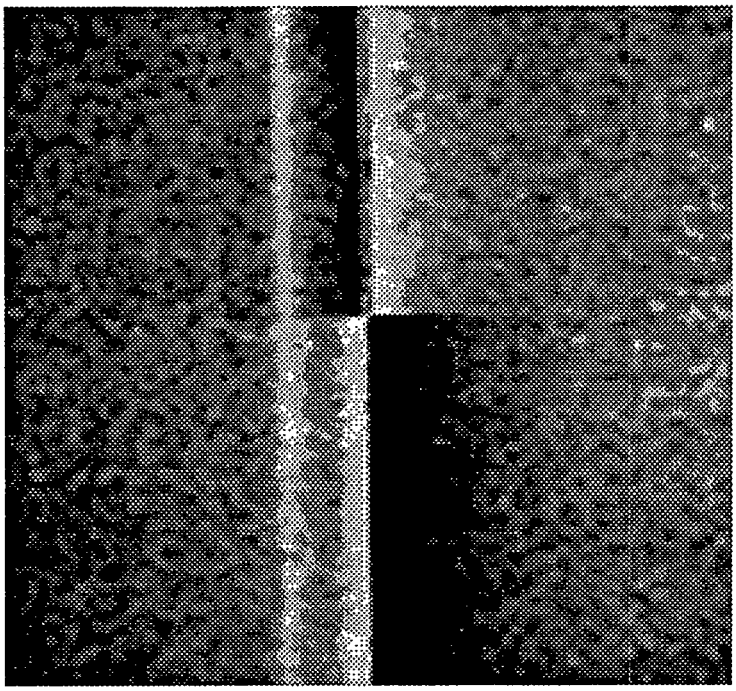

Figure 11. MFM image of the test structure with 20 μA ac current applied during the raster scan.

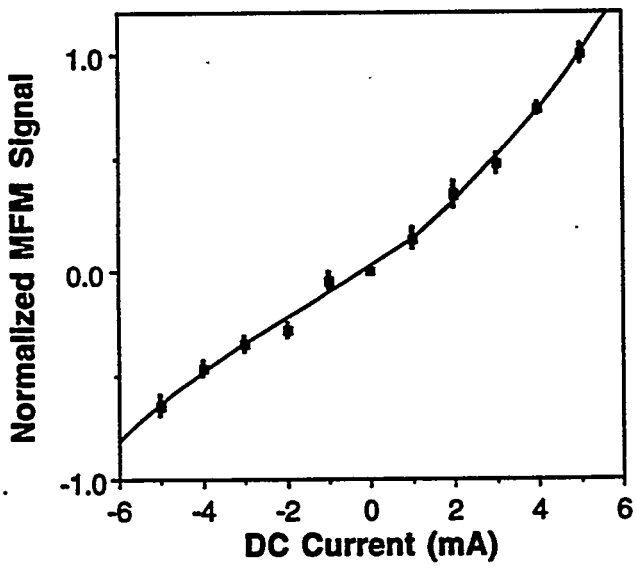

Figure 12. Plot of normalized MFM signal as a function of applied dc current.

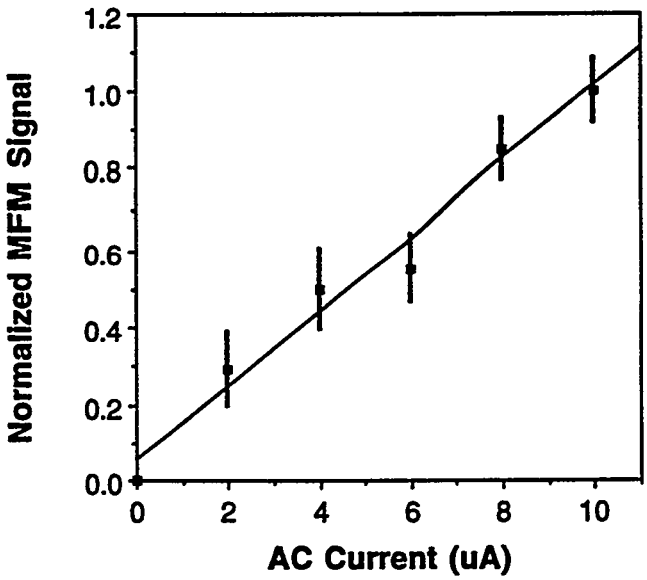

Figure 13. Plot of normalized MFM signal as a function of applied ac current.

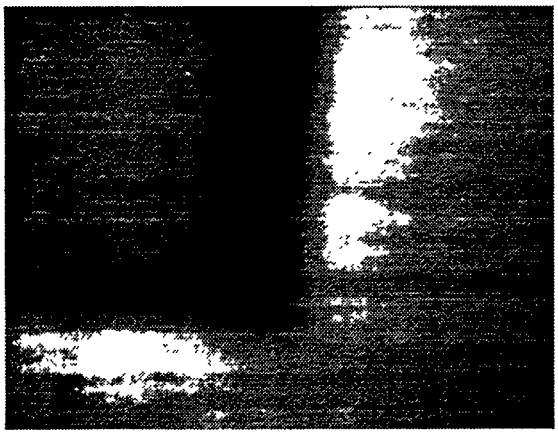

Figure 14. MFM current contrast image of the elevated current path on a damaged IC. Conductor location coincides with the bright/dark transition.

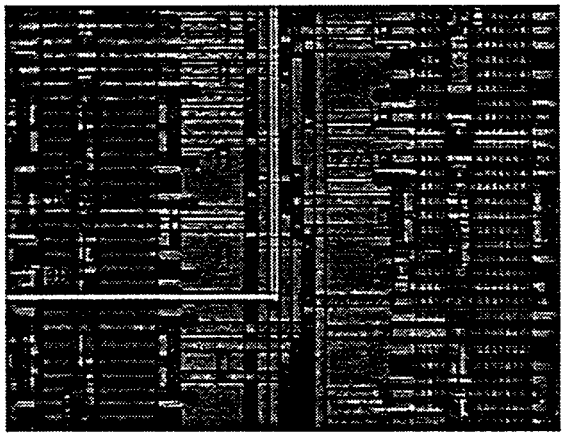

Figure 15. Optical micrograph of the same field of view as Figure 14, with the current path highlighted in white.

Figure 16. MFM current contrast image of the elevated current path on a damaged IC, ac mode imaging.

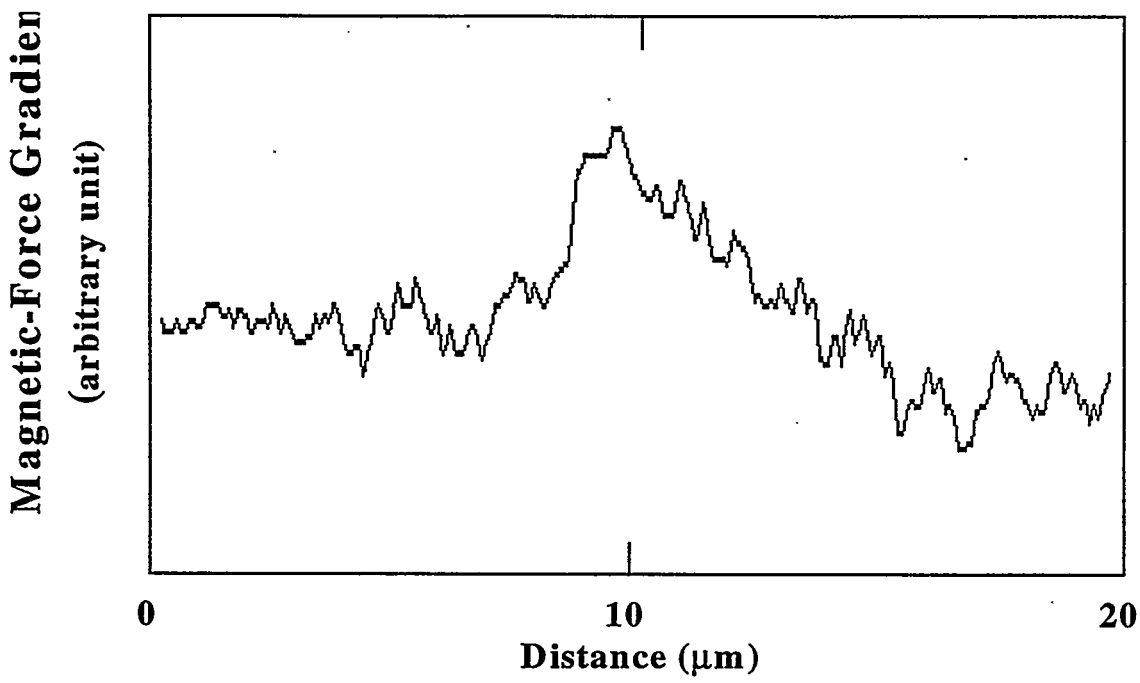

Figure 17. Experimental magnetic force gradient profile across an 8 μm wide conductor with 100 mA dc current. The profile was measured with a thin-film magnetic tip.

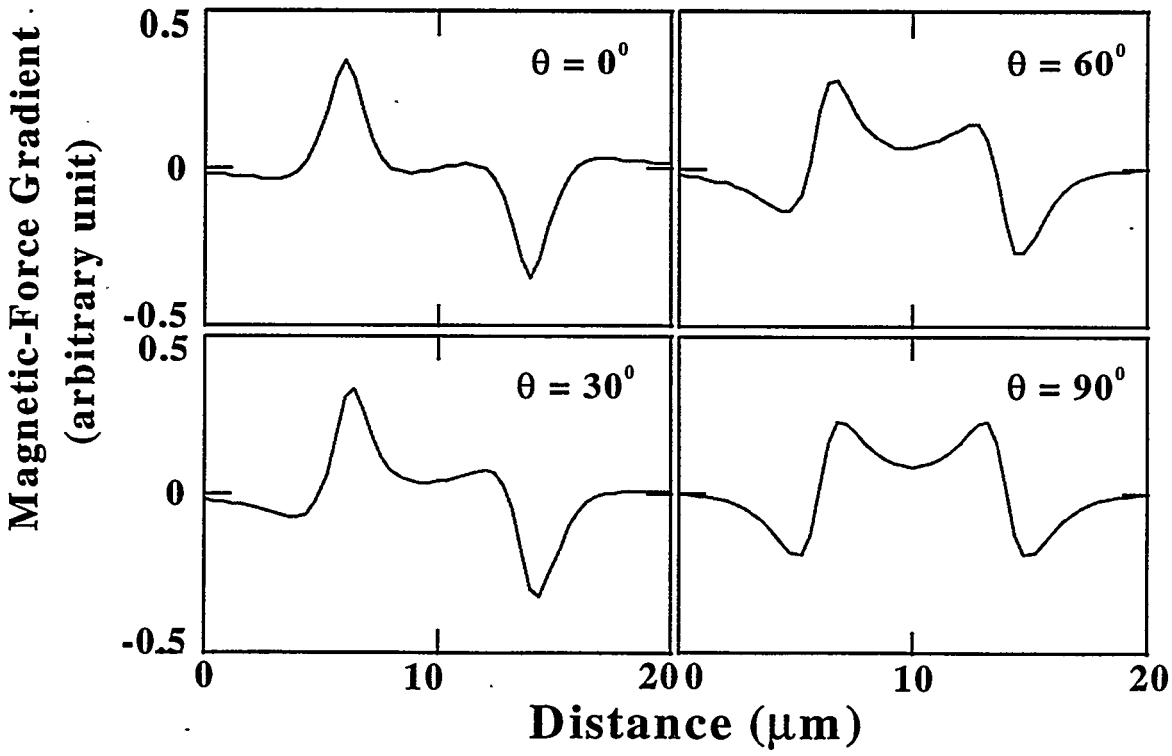

Figure 18. Simulations of magnetic force gradient profiles across an 8-μm-wide conductor assuming different orientations of the tip magnetic dipole moment with respect to the surface normal.

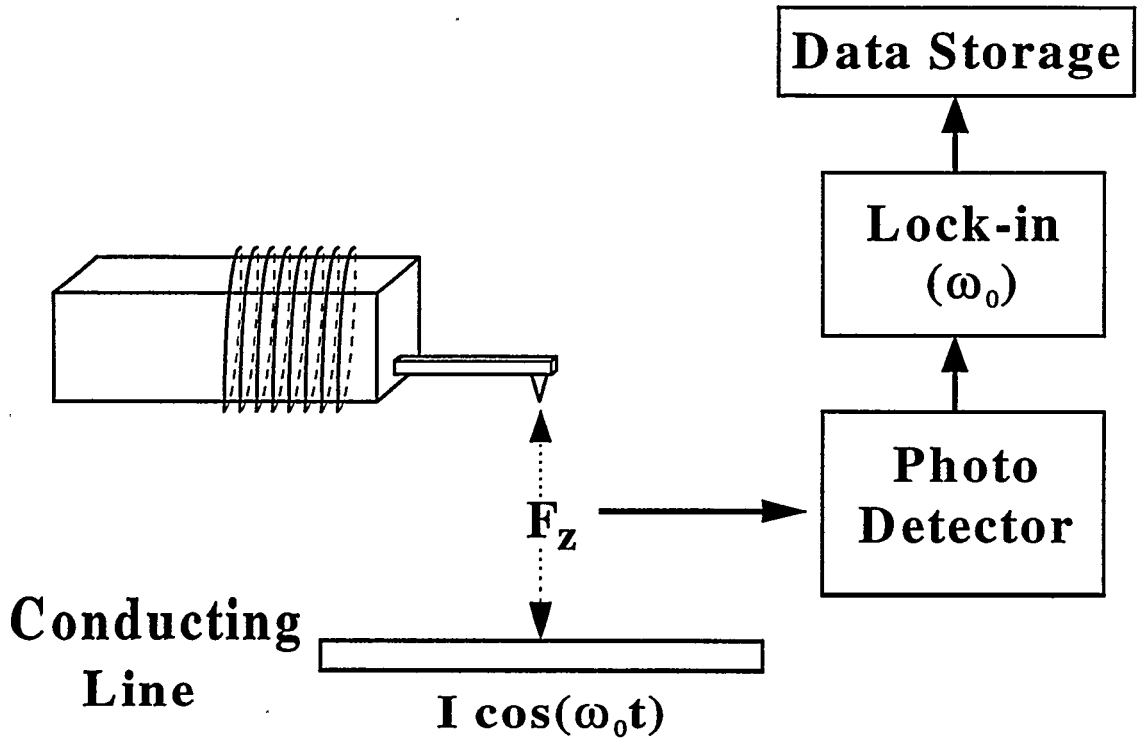

Figure 19. Experimental setup for measuring magnetic force profiles across a conductor.

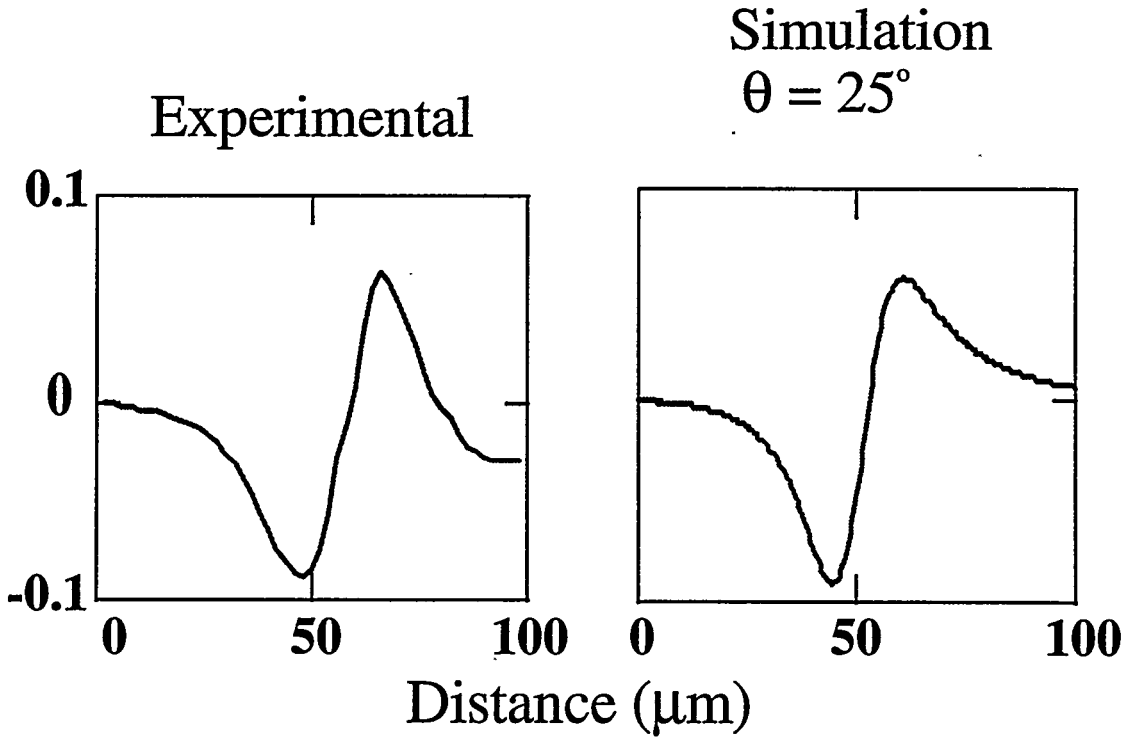

Figure 20. Comparison of simulated and experimental magnetic force profiles across a conductor.

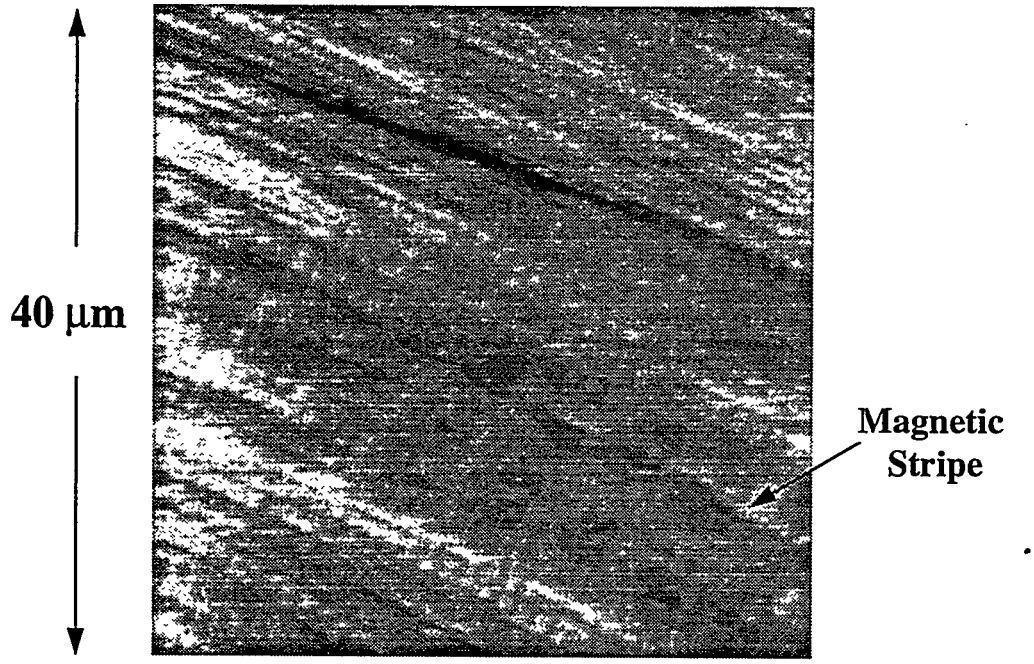

Figure 21. An MFM image of a magnetic disk taken with a tip-sample separation of ~ 10 nm using a weakly magnetized tip. The image consists mostly of topographic information with a series of weak magnetic stripes (indicated by an arrow).

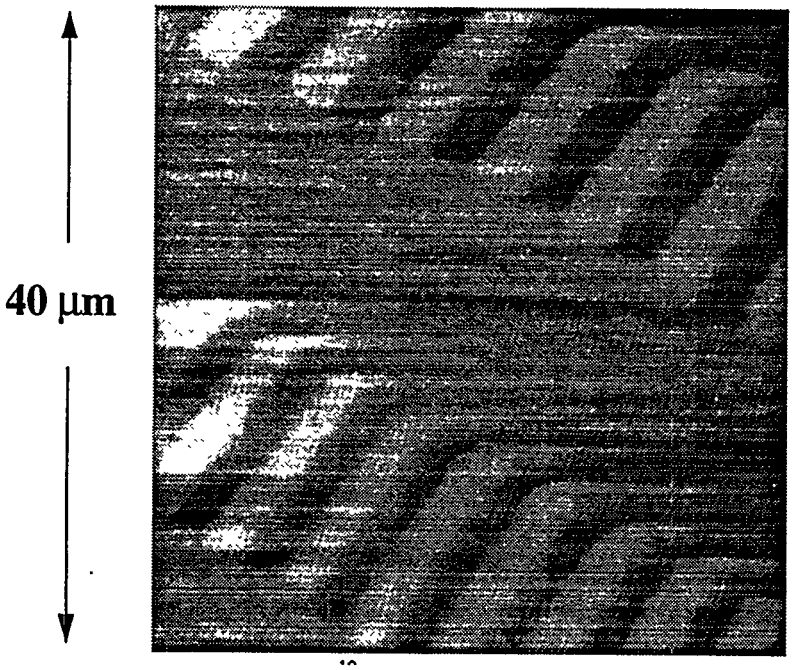

Figure 22. An MFM image of a magnetic disk taken with a tip-sample separation of ~500 nm after remagnetization of the tip. The image clearly shows a series of strong magnetic stripes.

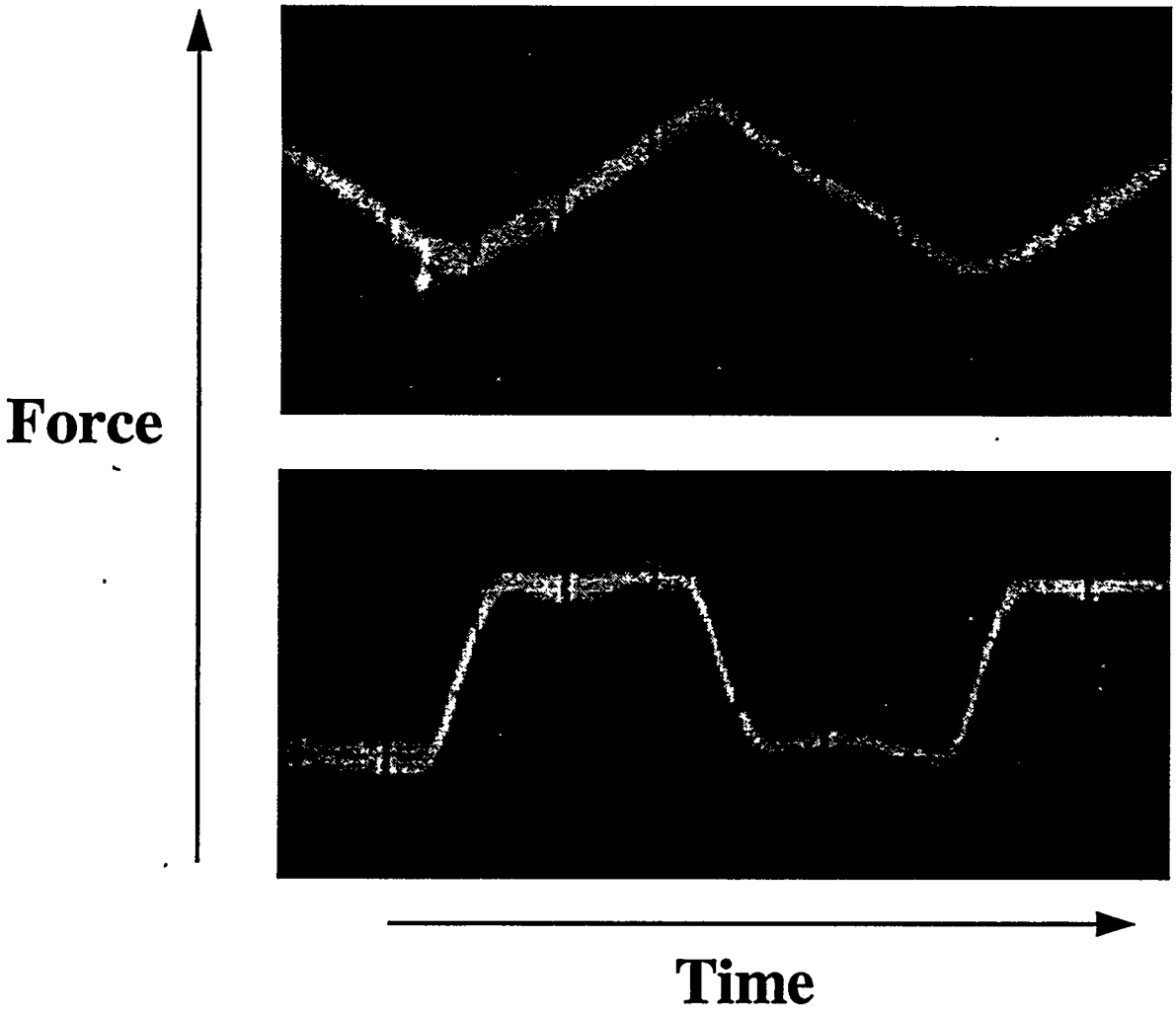

Fig. 23 Oscilloscope displays (Ω = 100 Hz) showing the magnetic force between a magnetic thin-film tip and a conductor as a result of passing ac currents through the solenoid placed around the base of the cantilever.

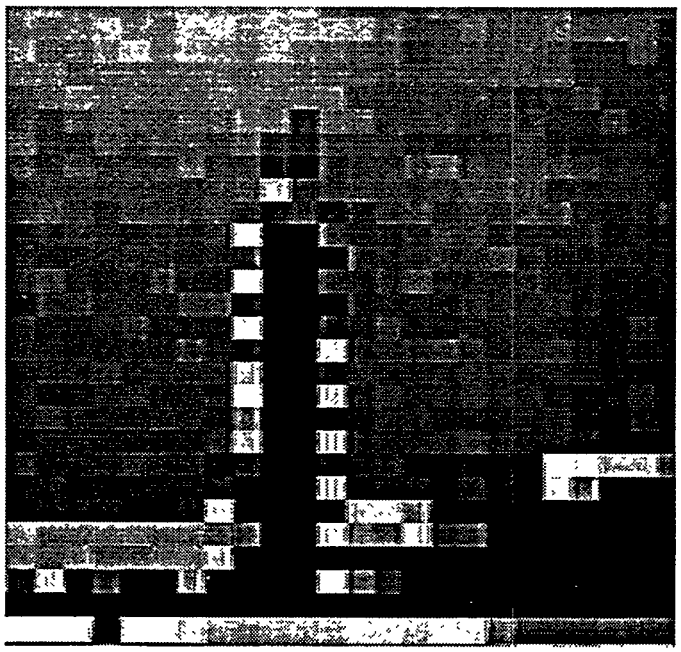

Figure 24. Large area (600 μm x 220 μm) magnetic force image of a 20 mA ac current through an IC conductor.

EVALUATION OF PROGRESS TOWARD GOALS AND MILESTONES

The goal of this LDRD project was to develop and refine SPM techniques for measuring currents in and voltages on internal conductors of operating ICs for the purposes of IC failure analysis, design verification, and model validation. In this two-year project, the first year was intended to demonstrate proof-of-concept and the second year would focus on refinements of the techniques. Our goals were to achieve current sensitivity of 1 μA with a spatial resolution of better than 1 μm and voltage sensitivity of 1 μV with the same 1 μm spatial resolution. Our ten milestones were:

(1) Achieve non-contact mode imaging capability for our SPM
(2) Achieve MFM and CFM capabilities
(3) Develop 2-D model for the magnetic fields above typical IC conductor geometries
(4) Produce magnetic and conductive tips for MFM and CFM analysis
(5) Demonstrate current imaging on a simple test structure
(6) Demonstrate voltage imaging with STM and CFM on a simple test structure and determine signal resolution
(7) Demonstrate MFM and CFM on multiple conductors and determine signal resolution
(8) Demonstrate MFM and CFM on full-up ICs in static bias
(9) Construct mosaic of smaller images for larger IC area analyses
(10) Produce a final (SAND) report.

During the first year of the project we developed and demonstrated proof-of-concept for the MFM/CCI technique and also began experimenting with voltage imaging. We continued working to refine both current and voltage imaging in the second year. We demonstrated current imaging with 1 μA sensitivity during the first project year, and achieved submicron spatial resolution for both current and voltage probing during the second year. We did not meet our goal of achieving precise potentiometry with μV sensitivity because, as explained in the following paragraph, STM proved to be an unreliable technique for probing unpassivated aluminum conductors. We did implement voltage probing with CFM and achieved 10 mV sensitivity, which is within an order of magnitude of that reported by other workers [17]. Primary emphasis in the second year was placed on developing improved sensors for MFM/CCI. Some of our milestones were modified during the project in response to technical developments as explained below.

This two year project consisted of eight quarters. Our first milestone, implementation of non-contact mode imaging for our SPM, was achieved during the first quarter. The second milestone, achieving MFM and CFM capabilities, was reached by the end of the first quarter for MFM and by the fourth quarter of the project for CFM. Development of a two-dimensional model for magnetic fields above typical IC geometries was achieved by the end of the second quarter. Milestone four, production of magnetic and conductive tips for MFM and CFM, was achieved within the first quarter for MFM and in the fourth quarter for CFM. In addition, we continued to refine our techniques throughout the project. Milestone five, to demonstrate current imaging on a simple test structure, was achieved within the first quarter, developed during the first year of the project, and refined in the second. Milestone six, to demonstrate voltage imaging with STM and CFM on a simple test structure, was achieved during the second year for imaging with CFM. The approach using STM was abandoned for two reasons: first, other workers reported difficulties

achieving repeatable potentiometry results on aluminum conductors due to the aluminum oxide at the surface; and second, typical IC structures are covered with insulating materials (passivation) which would prevent using STM as a non-invasive probe except at bond pads (and, due to the aluminum oxide at the surface, those results would probably not be reliable). Demonstration of MFM and CFM on multiple conductors and determining signal resolution (milestone seven) was achieved during the second project year. Milestone eight was to demonstrate both techniques on ICs with static bias. We fulfilled this milestone in part by demonstrating that MFM/CCI could localize failures on several different ICs with static bias. The limitations encountered with the non-contact mode operation on our system (tip crashes and difficulty in accommodating large packages) complicated the application of MFM/CCI on our present SPM platform. The experiments performed on the new Digital Instruments Dimension 3000 system (which became available during the last quarter of this project) demonstrated that the new SPM platforms will allow these experiments to be performed much more easily, but time did not permit us to complete milestone eight on that system. Milestone nine called for constructing a mosaic of smaller area images to generate a large area image. This milestone was modified to the goal of achieving large area scanning, which was demonstrated during the fourth quarter of the project. This approach will be of much greater utility in diagnosing IC failures and quickly localizing elevated current paths on an entire IC. Large area scanning will be considerably more economical in terms of both image acquisition time and computed image memory (one image will be acquired, rather than many required for mosaicking). In addition, the large area scanning approach had not been tried before, while the technology for mosaicking has already been developed and does exist in our laboratory if the need arises to obtain a mosaicked image. Finally, milestone ten calls for the preparation of a final SAND report; this document achieves that goal.

As this summary describes, we have met almost all of our milestones and goals. Where we did not meet or modified them, we have described the reasons.

PUBLICATIONS AND AWARDS

1. A. N. Campbell, E. I. Cole, Jr., B. A. Dodd, and R. E. Anderson, "Internal Current Probing of Integrated Circuits Using Magnetic Force Microscopy", 31st Annual Proceedings of the International Reliability Physics Symposium, 168 - 177 (1993). *This paper received the International Reliability Physics Symposium 1993 Outstanding Paper Award, presented April 13, 1994 in San Jose, CA.*

2.) A. N. Campbell, E. I. Cole, Jr., B. A. Dodd, and R. E. Anderson, "Magnetic Force Microscopy/Current Contrast Imaging: A New Technique for Internal Current Probing of ICs", Microelectronic Engineering **24**, 11 - 22 (1994). *This was an invited paper, presented at the 4th European Conference on Electron and Optical Beam Testing in Zurich, Switzerland, September 1 - 3, 1993.*

PATENTS AND INTELLECTUAL PROPERTY

A patent application titled "Magnetic Force Microscopy Method and Apparatus to Detect and Image Currents in Integrated Circuits" was filed with the United States Patent & Trademark Office on March 21, 1994 and assigned Serial No. 08/215,431. The Sandia-assigned numbers are SD-5394; S-80,842.

In May 1994, Ann Campbell was contacted by a small business that expressed strong interest in licensing the MFM/Current Contrast Imaging technology. Org. 4211 decided that it would be prudent to place an advertisement in Commerce Business Daily before committing to a particular commercial partner. A press release was also prepared on the technology, and as a result articles appeared in a number of publications, including Business Week (10/10/94), R&D Magazine (11/94, p. 18 - 19), Nasa Tech Briefs (11/94), The Federal Lab Test & Measurement Tech Briefs (11/94), Design News (10/24/94, p. 13), Electronic Design (10/25/94, p. 27), Electrical Engineering Times (10/3/94, p. 39), Sandia Science News (11/94), and The Sandia Lab News (9/30/94, p. 8).

Sandia has received a number of interested inquiries, including from several scanning probe microscope manufacturers and from potential users of a commercial system. At present, Sandia has one licensing agreement in place and is pursuing a second for this technology.

SYNERGISTIC WORK

During FY 94 we began a Work for Others (WFO) project that is based on and synergistic with the work performed under this LDRD. The project involves the development of a technique for SPM-based current waveform detection and has continued in FY 95 at a 1.0 FTE rate.

POTENTIAL FUTURE WORK & INTERACTIONS

The technology developed under this LDRD has been met with great enthusiasm from the IC analysis community. Department 2275 presently has a CRADA under negotiation with

a company interested in licensing this technology. In addition, we are discussing additional WFO projects with our Org. 5900 customers as a direct outgrowth of this LDRD project.

BENEFITS TO DOE DEFENSE PROGRAMS (DP)

This LDRD project has benefited DOE Defense Programs by developing a new technology for non-invasive detecting and imaging of currents in IC conductors for IC failure analysis, design verification, and model validation. This technology is resident in Sandia National Laboratories Failure Analysis Deparment 2275 and can be used for Stockpile Support and the development of new DP systems and programs (such as MDE).

HIRING OF PERMANENT TECHNICAL STAFF

As a result of the new business generated from our technical accomplishments under this LDRD project, Department 2275 was able to add one additional permanent staff member (Paiboon Tangyunyong, SMTS).

DISTRIBUTION

MS 0320	C. E. Meyers, Org. 1011	(2)
MS 1070	R. E. Bair, Org. 2200	(1)
MS 1071	T. A. Dellin, Org. 2203	(1)
MS 1071	T. J. Allard, Org. 2205	(1)
MS 1081	R. E. Anderson, Org. 2275	(1)
MS 1081	A. N. Campbell, Org. 2275	(5)
MS 1081	E. I. Cole Jr., Org. 2275	(1)
MS 1081	P. Tangyunyong, Org. 2275	(1)
MS 0344	T. A. Michalske, Org. 1114	(1)
MS 0344	J. E. Houston, Org. 1114	(1)
MS 0603	L. Griego, Org. 1322	(1)
MS 0603	A. J. Howard, Org. 1322	(1)
MS 0956	M. Gonzales, Org. 2412-1	(1)
MS 9018	Central Technical Files, Org. 8523	(1)
MS 0899	Technical Library, Org. 13414	(5)
MS 0619	Print Media, Org. 12615	(1)
MS 0100	Document Processing Org. 7613-2 For DOE/OSTI	(2)